# Processing the Raman Spectrum using Wavelets and Neural Network to Diagnose Human Basal Cell Carcinoma

**Alderico Rodrigues de Paula Júnior**
UNIVAP – 12 244-000 Av. Shishima Hifumi 2 911, São José dos Campos, Brazil
alderico@univap.br

**Airton A. Martin**
UNIVAP – 12 244-000 Av. Shishima Hifumi 2 911, São José dos Campos, Brazil
amartin@univap.br

**Herculano da Silva Martinho**
UNIVAP – 12 244-000 Av. Shishima Hifumi 2 911, São José dos Campos, Brazil
hmartinho@univap.br

***Abstract.*** *Raman spectra from normal and malignant Han (Basal Cell Carcinoma) skin were acquired using an Nd: YAG laser at 1064nm, as the excitation source, in the FT-Raman spectrometer. Fifty-three sets of human skin samples composed of 20 tissues histopathologically diagnosed as non-diseased, and 33 tissues diagnosed as Basal Cell Carcinoma, were obtained. Analyzing the Raman spectra it was verified that the spectral region that better differentiated the two types of tissues was from 800 to 1400 cm$^{-1}$. It was also observed that the information in the selected spectral bands had a high level of redundancy. Different processing algorithms for compressing the acquired signal and data classification were analyzed. The discrete wavelet transformation was selected for the data compression phase and the neural network for the classification phase. Different compression ratio and different neural network topologies were analyzed. The best result was reached when a neural network having four neurons in the first hidden layer and two neurons in the second hidden layer was combined with the wavelet transform with a compression ratio of 1 to 16. The developed algorithms were found to provide promising diagnosis results with no classification errors. It has been concluded that the developed algorithms would be very useful in the development of Raman spectroscopy systems for in vivo biological applications.*

**Keywords :** *Raman spectroscopy, Basal cell carcinoma, Discrete wavelet transform, Artificial neural network.*

## 1. Introduction

Non-melanoma skin cancers are the most common forms of malignant neoplasm in humans. The majority of the cases are diagnosed as basal cell and squamous cell carcinomas (Alam and Ratner, 2001, Altman, 2000 and Sigurdsson 2004). Basal cell carcinoma (BCC) is the most frequently diagnosed skin cancer, accounting for approximately 75% to 80% of all reported cases.

All disease states are caused by fundamental changes in cellular and/or tissue biochemistry (Mahadevan-Jansen, and Richards-Kortum, 1996 and Mahadevan-Jansen and Richards-Kortum, 1997). The qualitative analysis of such biochemical changes may provide important clues in the search for a specific diagnosis. The quantitative analysis of biochemical abnormalities is important to determine the extension of the disease process, to design therapy and to evaluate the efficacy of treatment.

The conventional method for tissue analysis is the histopathological examination of biopsy samples. However, histopathological diagnosis utilizes morphologic abnormalities rather than biochemical differences identified by the pathologist on a subjective basis. Furthermore, pathological analysis requires tissue to be removed, with undesirable consequences. In addition, conventional histopathology lacks both the capabilities of providing immediate feedback and the precision to quantify the extension of the disease, particularly in the early stages. For these reasons, *in loci* techniques that provide real-time and quantitative information about tissue biochemistry are under study to help histochemical examination of biopsy specimens (Manoharan,,Wang and Feld, 1996 and Schrader et al., 1999).

Many physical methods for *in situ* tissue analysis have been explored, but the molecular investigation by vibrational spectroscopy has a number of advantages over other methods, including minimal or no damage to the sample. Raman spectroscopy, which had earlier been used extensively for investigating chemical compounds, has recently emerged as a tool for characterization of the molecular structure of normal and diseased tissues (Nunes et al., 2003 and Schut, et al., 2000). The principle of Raman spectroscopy was started in 1928 when Chandrasekdara Raman observed that when a sample is irradiated with monochromatic light, new lines are present in the spectrum of scattered light, the frequencies of which reflect vibration of molecular bonds in the examined samples. This phenomenon allows on analyzing the molecular structure of compounds by means of their spectral fingerprints (Kaminaka et al., 2002). Raman spectroscopy is a nondestructive analytical method (no mechanical decomposition, no chemical decomposition, no photochemical decomposition, no thermal decomposition) for determining the structure and conformation of molecular compounds. It

does not require sample preparation or pretreatment. The advantage of the FT-Raman technique is that minimal fluorescence is produced making detection of the weak Raman signal easier.

In this work, different algorithms to process signal acquired by FT-Raman spectroscopy are investigated aiming to detect the alterations in the molecular structure that occurs in Basal Cell Carcinoma compared to the normal skin. The purpose of the present study is to determine an acceptable compression ratio for the preprocessed vector and an artificial neural network topology that provides satisfactory tissue classification results.

## 2. Material and Methods

Basal Cell Carcinoma was obtained from 21 patients of a "Municipal Family Health Unit" in São José dos Campos, São Paulo, Brazil who presented suspect lesions during physical examination. Non-diseased skin samples were obtained from plastic surgery at the aforementioned institution. Each sample was divided into two slices, one slice was sent to the histopathologist and another for spectroscopic study. The samples were collected soon after the surgical resection, identified and stored in liquid nitrogen (-196$^{o}$ C) until the moment of FT-Raman spectra recording.

This research was done according to ethical principles, following research norms of regulation with human beings, in accordance with resolution n.196/96 of the National Council of Health and was approved by The Ethical Commission in research of the Municipal Health system of São José dos Campos and by the Valley of Paraíba University (UNIVAP – Universidade do Vale do Paraíba). Patients were informed of the research and permission was given for samples used.

All skin samples were snap frozen and stored in liquid nitrogen (-196ºC) in cryogenic bottles at the Laboratory of Biomedical Vibrational Spectroscopy - IP&D, Institute of Research and Development, UNIVAP.

### 2.1. Equipment

A FT-Raman spectrometer (RFS 100/S – Bruker Inc., Karlsruhe, Germany) was used with an Nd: YAG laser at 1064nm as excitation source. Power output was 300mW and data was obtained with 250 scans at a resolution of 4cm$^{-1}$. A Ge detector collected Raman signals.

### 2.2. FT-Raman spectroscopy

For collection of FT-Raman data, samples were brought to room temperature, placed in a windowless aluminum holder and moistened with 0.9% physiological solution to preserve their structural characteristics. The Raman spectrum collecting time was approximately 4 to 6 minutes. One or two different points had been chosen by visual examination as the most important clinical aspects of the tissue. One spectrum per sample smaller than 3mm, and two spectra per sample larger than 3mm were collected.

Fifty three Raman spectra, 20 for non-diseased samples, and 33 BCC samples were collected. To prevent degradation and dehydration of the samples during analysis, they were periodically moisturized with 0.9% physiological solution. Soon after the FT-Raman spectra collection, the samples were immersed in a 10% formaldehyde solution and later submitted to histopathological analysis.

## 3. Data Analysis

In this article, vectors are represented by lower case boldface letters and matrices by upper case boldface letters. The subscripted letter T after the vector or matrix name indicates the transpose of the matrix or vector. The signal collected by the FT-Raman spectrometer is formatted to a 623 element vector, $\mathbf{x} \in R^{1x623}$. Each vector element represents the intensity of the radiation received from a particular spectral band position. Then, the t test was applied to the 623 variables of the formatted vectors in order to determine in which spectral bands the BCC tissue mean differed with significance level greater than 0.05 from the normal tissue mean generating the vector SD. This vector, when in high level, indicates that the means were significantly different. The average vectors of each tissue type and the vector SD are presented in Fig. 1.

It can be observed in Fig.1 that the range from 800 to 1400 cm$^{-1}$ significantly differentiates the two tissue types. This region, composed of 320 spectral bands, was selected for the next phase of the study.

### 3.1. Processing Techniques

Different techniques for processing the Raman Spectra and their classification into pathologic or non-pathologic tissues were investigated. The techniques analyzed for data compression were the Principal Analysis Component (PCA) and the Discrete Wavelet Transform (DWT) and, for classification, the Mahalanobis Distance Classifier (MDC) and the Artificial Neural Network (ANN). The methods that presented the best classification results were a combination of the wavelet transformation to compress the input vector and the neural network for classification.

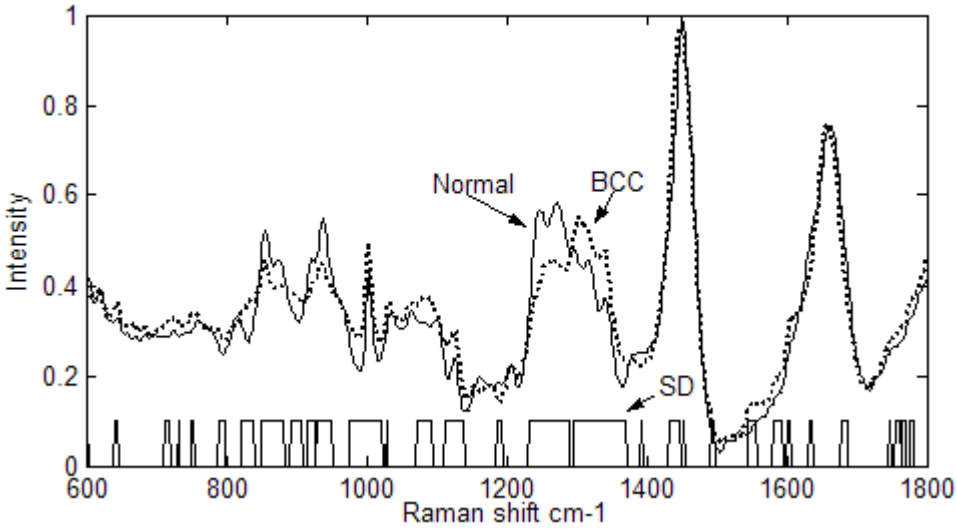


Figure 1 Comparison between BCC and normal skin spectral band means.

Artificial neural networks (ANNs) are computational algorithms appropriate for complex classification and pattern recognition problems. Similar to human mind, the neural networks are implemented using simple nonlinear or linear processing elements, named neurons, which may interconnect with each other ones forming complex processing networks. These networks may be trained adjusting the interconnection branch loads (synaptic weights) through training algorithms. After trained, the ANN can be used to perform certain tasks depending on the particular application. Different types of neural networks are described in the literature (Haykin; 1999). For pattern recognition problems, the most commonly utilized type is the multilayer feedforward perceptron (MPL) network. This class of network is composed of one input layer that receives the vector to be classified, one output layer that presents the classification results and a set of intermediate layers named hidden layers. The number of intermediate layers and the number of neurons in each intermediate layer depend on the complexity of the problem to be solved. Fig. 2 presents a feedforward neural network having ten inputs, a hidden layer with four neurons and an output layer with two neurons.

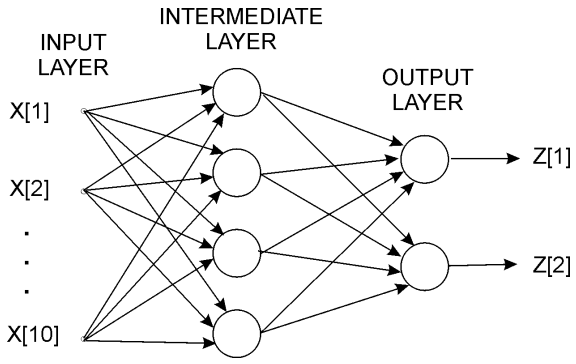


Figure 2. A multilayer feedforward neural network

The ANN frequently presents better classification results when the input vector is compressed to decrease the number of variables, to filter the noise and to maximize some features that facilitate the classification phase. The dimensionality reduction technique selected for this work was the discrete wavelet transformation (DWT).

The DWT (Kaiser, 1999 and Mallat, 1999 ) is a linear transformation represented by a matrix $\mathbf{H_N} \in R^{NxN}$ that transforms the input vector $\mathbf{x} \in R^{1xN}$ into a new vector $\mathbf{w}$ of the same length as $\mathbf{x}$, that may be computed by the following equation: $\mathbf{w^T} = \mathbf{H_N}.\mathbf{x^T}$. The odd rows of $\mathbf{H_N}$ contain the low frequency wavelet coefficients, while the even rows, the high frequency wavelet coefficients. The resultant vector $\mathbf{w}$ can be split into two vectors: $\mathbf{w_l} \in R^{1 \times N/2}$ (low-pass filter followed by dyadic decimation) that contains the low frequency components or averages and $\mathbf{w_h} \in R^{1 \times N/2}$ (high-pass filter followed by dyadic decimation) that contains the high frequency components or the details. The matrix $\mathbf{H_N}$ can be decomposed into the matrices, $\mathbf{H_{LN}} \in R^{N/2 \times N}$ that directly generates the low frequency vector $\mathbf{w_l}$ and the matrix $\mathbf{H_{HN}} \in R^{N/2 \times N}$ that directly generates the high frequency vector $\mathbf{w_h}$. The variable number reduction method consists in keeping the vector $\mathbf{w_l}$ and discarding the vector $\mathbf{w_h}$ resulting, in this way, a compression factor of 2 to 1.

When N is odd, $\mathbf{H_{LN}}$ may be adjusted to generate M element vector, where M is the smallest integer number greater than N/2. In order to achieve a greater compression factor, the DWT may be applied successively: initially on the input vector of length N, then on the resultant N/2 average vector and so on until the desired compression level is achieved. The compressed vector from the ratio N to (N/n), n={2, 4, 8, 16, ...}, may be computed in one step by the matrix $\mathbf{H_L^{N/n}}$ generated by the multiplication of low frequency matrix of each level.

Different wavelet families were analyzed (Peris and Paula, 2000 ). One wavelet that presented suitable for the current application was the Daubechies with four coefficients. Fig. 3 presents the original (preprocessed) Raman spectrum from a BCC tissue shifted by two in y-axis direction, the compressed signal into the ratio of 1:4 shifted by one and the compressed signal into the ratio 1:16.

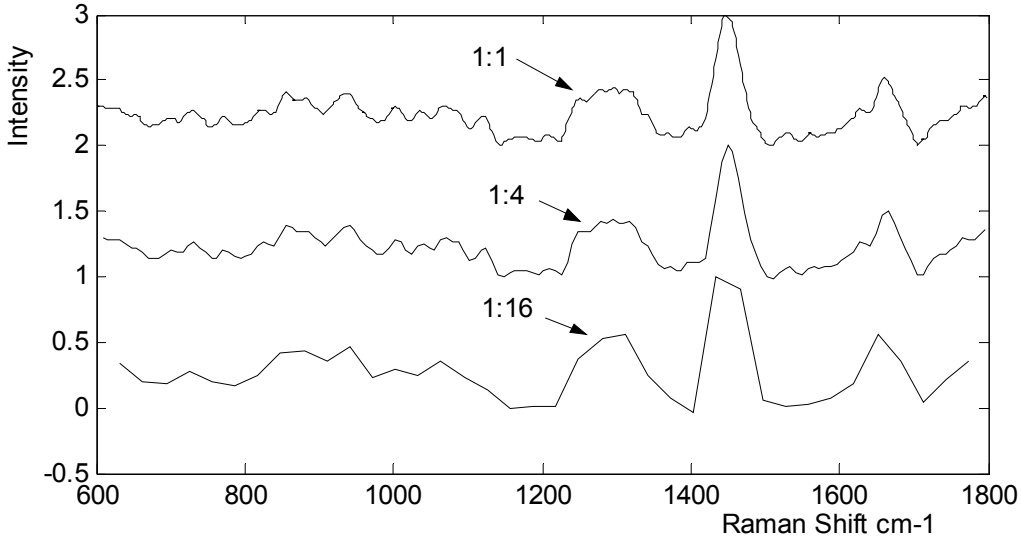


Figure 3. A Raman spectrum of a BCC tissue before and after being compressed

The compression phase based on the DWT can be viewed as the input layer of ANN which neurons have the linear transfer function.

### 3.2. Training and Validation Matrices

In order to compare the compression ratio and classification techniques, a total of 53 spectra acquired from human normal and BCC tissues were organized into two groups. The first group, formed by 12 spectra from normal tissue and 22 from pathologic tissue, constituted the training matrix $\mathbf{X} \in R^{34 \times 623}$. The second group having 8 spectra from normal tissue and 11 from pathologic tissue constituted the validation matrix $\mathbf{Y} \in R^{19 \times 623}$. All spectra of the matrices **X** and **Y** were filtered using a pass-band zero-phase digital filter and their amplitude adjusted between zero and one. Then, the elements of the normalized matrices corresponding to the spectral region from 800 to 1400 $cm^{-1}$ were selected for the next processing phase forming the matrices $\mathbf{Xs} \in R^{34 \times 320}$ and $\mathbf{Ys} \in R^{19 \times 320}$.

### 3.3. Spectral Compression

In the present study, three compression ratios were analyzed. The first ratio, 1:4, denoted W2, was reached by applying the selected DWT two times to all vectors of the matrices **Xs** and **Ys** forming the matrices $\mathbf{XW2} \in R^{34 \times 80}$ and $\mathbf{YW2} \in R^{19 \times 80}$ respectively. The second ratio, 1:8, named W3, was reached by applying the selected DWT three times resulting the matrices $\mathbf{XW3} \in R^{34 \times 40}$ and $\mathbf{YW3} \in R^{19 \times 40}$and, finally, the last ratio 1:16, denoted W4, was reached by applying the selected DWT four times producing the matrices $\mathbf{XW4} \in R^{20 \times 34}$and $\mathbf{YW4} \in R^{20 \times 19}$.

### 3.4. Classification Using Neural Networks

One of the goals of the chosen classification method was the selection of a low complexity neural network having a good capacity of generalization. As the number of classification groups was two (BCC tissue and non-pathologic tissue), the number of neural network outputs layer was defined to be one. For each training matrix, three feedforward neural network topologies with different complexity were analyzed. The first one (ANN-16-8) had 16 neurons in the first hidden layer and eight neurons in the second hidden layer. The second one (ANN-8-2) had also two hidden layers with eight neurons in the first layer and four in the second one. Finally, the last topology (ANN-4-2) had four neurons in

the first hidden layer and two in the second one. The selected neural network transfer function for the hidden layers was the hyperbolic tangent and for the output layer, the linear.

In order to have a good discrimination between the groups and an easy classification rule, the network desired outputs were selected according to Tab 1. In this table z[1] is the network output.

Table 1 Expected network outputs for each tissue category

| Tissue Type | z[1] | Classification Rule |
|---|---|---|
| BCC Tissue | -1 | z[1] <0 |
| Normal Tissue | 1 | z[1]≥ 0 |

The selected network training algorithm was the descent gradient having a learn rate of 0.05. To avoid the neural network becoming overfit, the network was trained until the mean square error between the desired values and computed values reached 0.001 or the number of training epochs reached 2000.

The training algorithm can provide different solutions for the same training matrix and for the same network topology depending on the initial synapse weights. In order to select an ANN for each one of the trained matrices that presented an adequate classification ratio, the training algorithm was executed 10 times for each of the proposed neural network topology. After trained, the validation matrices were utilized to evaluate the different topologies. To compare them, the ratio of the Euclidian distance between the ANN computed value and the desired correct group value and the Euclidian distance to the desired incorrect group value was computed for all vectors of the validation matrix. If this ratio is smaller than one the spectrum vector is correctly classified, else it is misclassified. Then, for each training matrix and each ANN topology the maximum distance ratio (MR) and the average distance ratio (AR) were computed. Among the ten networks generated by the training algorithm for the same topology having different synaptic weights, it was selected the network that presented the smallest maximum distance. Tab. 3 presents the correct classification ratio (CCR) in percentage, the maximum and average distance ratios for each selected ANN topologies and each training matrix. In this table, CR represents the compression ratio and ANN, the neural network topology.

Table 2. Correct classification ratio, maximum and average Euclidean distance ratios.

| CF | ANN | CCR | MR | AR |
|---|---|---|---|---|
| 1:4 | 16-8 | 100 | 0.39 | 0.13 |
| | 8-4 | 100 | 0.40 | 0.08 |
| | 4-2 | 83.7 | 5.39 | 0.71 |
| 1:8 | 16-8 | 100 | 0.47 | 0.16 |
| | 8-4 | 100 | 0.45 | 0.09 |
| | 4-2 | 100 | 0.29 | 0.06 |
| 1:16 | 16-8 | 100 | 0.42 | 0.06 |
| | 8-4 | 100 | 0.69 | 0.13 |
| | 4-2 | 100 | 0.23 | 0.04 |

As presented in Tab. 2, all the proposed ANN topologies except the topology ANN-4-2 with the compression rate of 1:4 correctly classified all the vectors of the verification matrix with a good safety margin. The best result was reached when the topology ANN-4-2 with the compression ratio of 1:16 was utilized. For this method, a low complexity neural network was utilized; the maximum distance ratio was 0.23 and the average distance rate 0.04 representing a very good margin. This indicates that spectrometer acquisition time may significantly decrease improving the time required for the diagnosis.

## 4. Conclusions

In this study, a digital processing method to classify the Raman spectra from BCC lesions and non-pathologic tissues was discussed. Initially, a band-pass zero-phased digital filter to remove the DC level was applied to filter the Raman spectra acquired from the tissues to be classified and to reduce the high frequency components composed mainly of the equipment noise. Then, the filtered signals were adjusted between zero to one. Analyzing the spectra from the normal and BCC tissues, it was verified that the spectral region that better differentiated the two types of tissue was from 800 to 1400 $cm^{-1}$ and, consequently, this spectral region composed of 320 spectral bands was selected for the classification phase. It was also observed that the information in the selected spectral band had a high level of redundancy and some techniques for dimensionality reduction could be used. The selected technique was the spectrum compression using discrete wavelet transformations. Three compressed ratios were utilized: W2 having a compress ratio of 320 to 80; W3 -– from 320 t0 40 and W4 – from 320 to 20. A set of 53 Raman spectra were acquired from non-pathological and BCC tissue and then preprocessed to reduce the noise and their dimensionality.

The 53 preprocessed spectra were divided into two groups: training matrices having 34 spectra and validation matrices having 19 spectra. The feedforward multilayer perceptron topology was selected for the classification phase. Different neural network topologies with two hidden layer were trained using the training matrices and then evaluated using the validation matrices. All the trained neural networks except the ANN-4-2 for the compress ratio of 1:4 classified correctly all spectra of the validation matrices with a good safety margin for the three compression ratios. The neural network with the smallest complexity composed of four neurons in the first hidden layer and two neurons in the second hidden layer combined with the wavelet compression ratio from 1 :16 was selected for the proposed application.

Finally, it can be concluded that the developed algorithms have an excellent potential for the development of Raman spectroscopy systems for *in vivo* biological applications, especially for BCC lesion diagnosis.

## 5. Acknowledgments

This work was partly supported by FAPESP (Research Support Foundation of the State of São Paulo- Brazil) through grant No. 01/14384-8 and by CNPq (National Research Council, Brazil) through grant 302393/2003-0. The authors would like to thank FAPESP and CNPq by the support received.

## 6. References

Alam, M. and Ratner, D., 2001, "Cutaneous squamous cell carcinoma", The New England Journal of Medicine, Vol. 344, No. 13, pp. 975-983.

Altman, J. F., 2000. "A survey of skin cancer screening in the primary care setting a comparison with other cancer screenings", Arch Fam Med, Vol. 9 No.10, pp. 1022-1022.

Haykin, S; 1999, "Neural Network: A Comprehensive Foundation"; Prentice Hall, Second Edition, New Jersey, 842 p.

Kaiser, G., 1999, "A Friendly Guide to Wavelets", Birkhäuser, Berlin, 300p.

Kaminaka, S. et al., 2002, "Near-infrared multichannel Raman spectroscopy toward real-time in vivo cancer diagnosis", J Raman Spectrosc, Vol. 33, No. 7, pp. 511-516.

Mahadevan-Jansen, A. and Richards-Kortum, R., 1996, "Raman Spectroscopy for the Detection of Cancers and Pre-cancers", Journal of Biomedical Optics, Vol.1, pp. 31-70.

Mahadevan-Jansen, A. and Richards-Kortum, R., 1997, "Raman Spectroscopy for cancer detection: A review Proceedings", 19th International Conference, pp.2722-2828,.

Manoharan, R., Wang, Y. and Feld M. S. , 1996, "Histochemical analysis of biological tissues using Raman spectroscopy", Spectrochimica Acta Part A - Molecular and Biomolecular Spectroscopy, Vol. 52, No.2, pp. 215-249.

Nunes, L. O et al., 2003, "FT-Raman Spectroscopy study for skin cancer diagnosi"; Spectroscopy, Vol. 17, No. 2 pp. 597-602.

Schrader, B. et al., 1999, "NIR Raman spectroscopy in medicine and biology: results and aspects"; Journal of Molecular Structure, Vol. 480, pp. 21-32.

Schut, T. C. B. et al., 2000, "In vivo detection of dysplastic tissue by Raman spectroscopy"; Anal. Chem.,Vol.72, pp. 6010-6018.

Sigurdsson, S. et al, 2004, "Detection of Skin Cancer by Classification of Raman Spectra", IEEE Transaction on Biomedical Engineering, No 10, Vol. 51, pp 1784 - 1793.

Mallat, S., 1999, "A Wavelet Tour of Signal Processing", Academic Press, 598 p.

Peris, C. M. F. and Paula Jr,. A.R., 2000, "Análise Comparativa de Filtros Wavelets para Processamento de Sinais Raman"; Workshop of Applied and Computational Mathematics, São José dos Campos, Brazil.

## 7. Responsibility notice

The authors are the only responsible for the printed material included in this paper.